Unsupervised Channel Charting with Channel State Information Using ULA and UCA Antenna Models in 5G Network

Jaakko Pihlajasalo Simo Ali-Löytty Mikko Valkama

{jaakko.pihlajasalo, simo.ali-loytty, mikko.valkama}@tuni.fi
Tampere University

Abstract

Channel charts are a map of the radio geometry that surrounds the base station and they are generated in an unsupervised manner from the received channel state information. In this work, we generate channel charts for two different antenna types for three different base station configurations. The method for generating the charts is explained, after which the results are shown and analysed.

1 Introduction

Fifth generation (5G) wireless systems make heavy use of large amounts of high dimensional uplink channel state information (CSI) [1] measurements acquired over large bandwidths and at fast rates from multiplicity of user equipment (UE) devices. To effectively use the CSI in enhanced communication functionalities, the network has to learn the geometry of the radio environment where the UE is moving. Hence, a chart of the radio geometry, which represents UE location and velocity related to CSI, can be beneficial.

In general, the charts should be able to tell whether the transmitters are close by or not. The chart should be generated only using the CSI measurements. This way the use of global navigation satellite systems (GNSS) systems, such as the global positioning system (GPS), and location fingerprinting campaigns can be avoided. In order to automate functions, learning of the chart should be carried out in an unsupervised manner. In this work, we apply the channel charting methods introduced in [2], where the tools of manifold learning, dimensionality reduction and multidimensional scaling are used to learn the chart.

In this work, we generate the charts for a uniform linear array (ULA) with 16 antenna elements and for a uniform circular array (UCA) with 20 antenna elements. For both antenna types, we use three different positions for the base stations in order to analyze the performance of the channel charting in a comprehensive manner.

This summary is structured as follows. In Section II, we describe the mathematical models used in the method. In Section III, the simulated scenarios and results are presented. In Section IV, we conclude the summary.

2 Channel charting

The goal of channel charting is to create a mapping from a CSI measurement $h \in \mathbb{C}^M$ to a point $z \in \mathbb{R}^2$ in a way that preserves the local geometry, that is, such that neighboring measurement locations map to neighboring points in the chart. Neighboring points in the real space are neighbors in the chart. To create the mapping, we define a dissimilarity metric that corresponds to the distance between users. The multicarrier-multiantenna CSI measurement h at the receiver has the dimensionality of $M = B \cdot W$, where B is the number of antenna elements in the antenna and W is the number of subcarriers in the considered orthogonal frequency-division multiplexing (OFDM)-based system. The dimensionality of z_n in this study is two, which matches the dimensionality of the position of the UE in real space projected onto a reference plane [2].

To acquire some knowledge between different antennas and subcarriers in CSI vectors, we the compute raw 2nd moment (R2M) of the CSI vectors. In practice R2M is computed as

$$\overline{H} = \frac{1}{T}\sum_{t=1}^{T} h_t h_t^H, \tag{1}$$

for small number of time instants T. Hermitian transpose is denoted as $(\,\cdot\,)^H$. The data is averaged over time to average out noise, interference and other potential variations caused by small scale motion. Before time averaging, subcarriers are also averaged, since the frequency response in the considered line of sight (LoS) propagation environment is almost flat, and thus does not significantly affect the overall performance. In addition, averaging helps with computation time and memory as matrices $\overline{H}$ have a dimension of $B \times B$.

Following [2], we extract channel features from $\overline{H}$ matrices in a two-step process. At the first step, a scaling is applied to compensate for path loss effects that distort spatial geometry. Due to path loss, users far from a base station tend to have smaller received signal power. The scaling transformation, which is intended to compensate for the path loss effect, is

$$\tilde{H} = \frac{B^{\beta-1}}{\|\overline{H}\|_F^{\beta}}\overline{H}, \text{ with } \beta = 1 + \frac{1}{2\sigma}, \tag{2}$$

where B is the number of antenna elements, parameter σ represents the path loss exponent, and $\|\cdot\|_F$ is the Frobenius norm. The path loss exponent σ is set to 16 in this study, as suggested by [2]. As the current goal is logical positioning rather than absolute, the factor $B^{\beta-1}$ can be omitted as it does not depend on different users and it only affects the distances in magnitude.

The second step is the application of nonlinearity to the scaled CSI matrices. By applying different nonlinearities, we obtain different features. For ULA antennas, we apply a two-dimensional discrete Fourier transform, then take the absolute value of the CSI matrices, as suggested in [2]. For UCA antennas, we test different transformations.

Finally, the CSI matrices after scaling and nonlinear transformation, denoted as F, can be used to compute the dissimilarity matrix, which is used to find the channel chart with Sammon's Mapping [3], a multidimensional scaling algorithm. Matrices F are either complex or real depending on the used feature. We use the Frobenius norm as a dissimilarity metric between the CSI matrices. The pairwise distance matrix $D \in \mathbb{R}^n$ of all channel features is computed with

$$D_{i,j} = d_f(F_i, F_j) = \|F_i - F_j\|_F, \text{ for } i = 1,...,n \text{ and } j = 1,...,n. \tag{3}$$

3 Simulations and results

In [2], the positions of the users are within a rectangular area. In our study, simulated data in a part of the METIS Madrid grid [4], which includes roads leading out from a rectangular area that represents a park (Figure 1). This shape is more realistic and the roads might affect the results significantly. We test three positions for the base station. The simulated users and the positions of the base station can be seen in Figure 1. The UE have been colored in the south-north direction. In this study, we only take LoS uplink CSI measurements into account, thus no base station has a direct line of sight to all of the users. Only the antenna in the corner scenario can see the roads visible in the figure.

In Figures 2, 3 and 4, we can see the results for ULA antennas for three different base station positions. The shape of the map is not preserved in the mapping process, which is expected. The shapes of the maps are somewhat similar to each other and to figures in [2]. The chart of the corner scenario (Figure 4) is slightly more distorted, probably because this location has a line of sight to users on roads. The local geometry seems to be well preserved, as the same colored points are grouped together and the gradient is continuous around the shape.

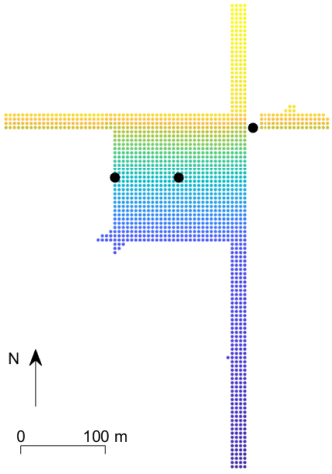

Fig. 1: Simulated UE positions with a color gradient indicating the northing coordinate. Base stations are shown as black dots.

The selection of the nonlinearity mapping for UCA antennas has to be done with trial and error, as the feature used for ULA antennas does not work with UCA antennas. There is no single feature that works well for all of the base station positions. Not applying any nonlinearity works the best for the scenarios with the antenna in the west and corner of park. For the antenna in the middle of the park taking the angle of the complex numbers works the best.

In Figures 5, 6 and 7, we see the best UCA charts for each of the base station positions. The chart has similar shape to ULA antenna results for west of the park and the corner of the park scenarios. The chart of the corner scenario is distorted as with ULA antenna. The middle of the park scenarios chart has a good color gradient and shape.

Even though the north to south color gradients look good, there might exist a symmetry that causes ambiguity. Symmetries can be recognized by coloring the charts in the east to west direction. If these colored points are mixed up, there is a symmetry. For the tested scenarios, we found a symmetry only in the middle of the park scenario for ULA antenna. This is likely due to the shape and position of the ULA antenna itself. The ULA antenna is positioned such that it receives measurements from both sides of the antenna, which can not be separated by only looking at the data. In other ULA scenarios, the antenna is next to a wall and the other side of the antenna can

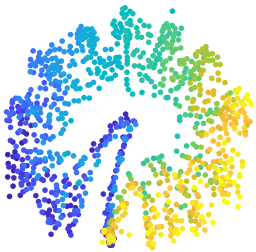

Fig. 2: Channel chart of ULA antenna west of the park

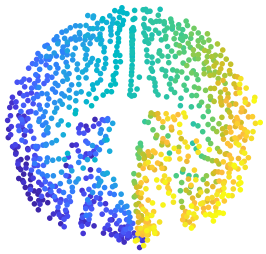

Fig. 3: Channel chart of ULA antenna in the middle of the park

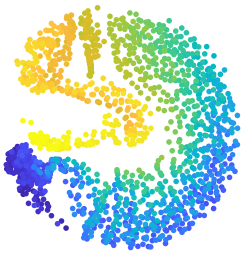

Fig. 4: Channel chart of ULA antenna north-east of the park

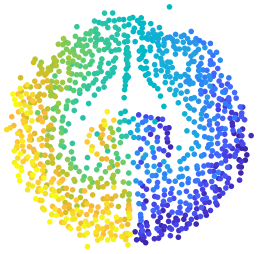

Fig. 5: Channel chart of UCA antenna west of the park

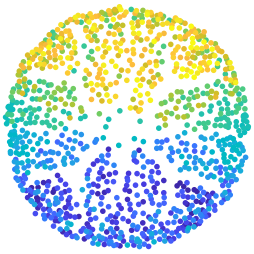

Fig. 6: Channel chart of UCA antenna in the middle of the park

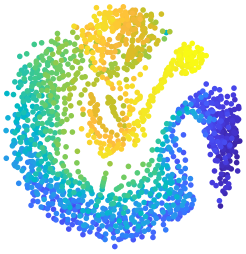

Fig. 7: Channel chart of UCA antenna north-east of the park

not receive any measurements or it receives less measurements.

4 Conclusions

The Channel Charting method presented in [2] was repeated for a few different scenarios as well as two different antenna types. We found that the type of the antenna affects the computation process and the charts. We have not found a single feature that works well for all scenarios. We found that the geometry of the area around the base station affects the chart, which can be seen in the distorted shape of the corner scenario charts.

Further research is needed for channel charting with multiple base station systems. ULA antenna results can possibly be improved with a different method that takes the symmetry into account. Both antenna types need more research to get a suitable method for all base station positions. The method needs improvement to get better shaped charts and estimation of absolute position. Locating the base stations from the charts is also of interest.

References

[1] A.Goldsmith *Wireless Communications*, Cambridge University Press, p. 102, DOI: 10.1017/CBO9780511841224 2005.

[2] C. Studer, S. Medjkouh, E. Gönültaş, T. Goldstein, and O. Tirkkonen *Channel Charting: Locating Users Within the Radio Environment Using Channel State Information*, IEEE Access. PP. 1-1. 10.1109/access.2018.2866979, 2018.

[3] J.W. Sammon *A Nonlinear Mapping for Data Structure Analysis*, IEEE Transactions on Computers. Volume: C-18 , Issue: 5, DOI: 10.1109/T-C.1969.222678, May 1969.

[4] METIS *D6.1 Simulation guidelines*, ICT-317669-METIS/D6.1, October 2013, available: https://www.metis2020.com/wp-content/uploads/deliverables/METIS_D6.1_v1.pdf.